Iraqi Journal of Physics, 2019 *Vol.17, No.40, PP. 88-94*
DOI: 10.20723/ijp.17.40.88-94

The dispersion in spherical statistical optical potential (SOM) from the interaction of fast neutrons with ^{197}Au nuclei

Fatimah Fadhil Abd Ali and Mahdi Hadi Jasim

Department of Physics, College of Science, University of Baghdad

E-mail: fatimamm39@yahoo.com

Abstract

A statistical optical potential has been used to analyze and evaluate the neutron interaction with heavy nuclei ^{197}Au at the neutron energy range (1-20 MeV). Empirical formulae of the optical potentials parameters are predicted by using ABAREX Code with minimize accuracy compared with experimental bench work data. The total elastic, absorption, shape elastic and total compound cross-sections are calculated for different target nuclei and different incident neutron energies to predict the appropriate optical parameters that suit the present interaction. Also the dispersion relation linking between real and imaginary potential is analyzed with more accuracy. The results indicate the behavior of the dispersion contribution in imaginary potential has a parabolic change about the Fermi surface energy while in the real potential it fall with increasing the neutron energy. Good agreements have been achieved with the available experimental data.

Key words
Spherical-statistical optical model, shape and compound elastic scattering, dispersion in real potential.

Article info.
Received: Sep. 2018
Accepted: Nov. 2018
Published: Mar. 2019

تشتت الجهد البصري الكروي الاحصائي من تفاعل النيترونات السريعة مع نوى االذهب 197

فاطمة فاضل عبد علي و مهدي هادي جاسم

قسم الفيزياء، كلية العلوم، جامعة بغداد

الخلاصة

تم استخدام النموذج البصري الكروي الاحصائي لحساب وتقييم التفاعل النيوتروني مع نوى ثقيلة ^{197}Au عند مدى طاقة النيوترون من 1 الى 20 ميجا الكترون فولت. تم حساب الصيغه التجريبيه لمعلمات الجهد البصري باستخدام شفرة ABAREX مع تقليل الدقه مقارنه مع البيانات العمل التجريبية و حساب المقطع العرضي (المرن، الامتصاص، الشكل المرن، المركب الكلي) لنوى الهدف و الطاقة النيوترونية مختلفه. كذلك تم تحليل وايجاد علاقة التشتت التي تربط بين الجهد الحقيقي والخيالي عند دقة عالية. وجد ان تاثير مساهمة التشتت في الجزء الحقيقي يتناقص مع زيادة الطاقة بينما الجزء االخيالي لدية اختلاف مكافىء حول طاقة سطح فيرمي. وقد تمت مقارنه النتائج مع الحسابات التجريبية.

Introduction

The SOM is one of the simplest and most successful models which are used to describe the elastic scattering of particle from nuclei. The solution to the complex many-body problem is approximated the interaction of two structureless particles through an effective potential. This represents by a complex potential, where both real and imaginary parts are energy dependent. The real part is referred to the refraction index while the imaginary part accounts for the absorption by the medium which described the formation of the compound nucleus. The imaginary part of the potential interacts with the incident wave and attenuates of the incident nucleon [1, 2]. The model was first proposed by Serber [3]

and used by Fernbach et al. [4] to calculate the probability scattering and absorption of 90 MeV neutrons by a range of nuclei. The SOM basis and starting point for all the nuclear model calculation which gives information about nuclear shape, nuclear structure and so on. The parameters are the main part and the knowledge of the model that play an essential role in the description of many nuclear reactions, e.g. inelastic scattering processes, transfer or the direct reactions, and in nuclear structure studies, the transmission coefficients and the inverse cross sections that used in statistical theory are also calculated with optical model [5]. The nuclear potentials are in general energy-dependent and nonlocal. The energy dependency of the real and imaginary parts of the optical model potential can be represented by a dispersion relation [6, 7].

Mahuaux and co-workers [8, 9] studied the nuclear reaction using the SOM containing dispersion in optical model relations (DOM), which connected the imaginary part with a corrected contribution to the real part of the model that follows from the requirement of causality principle scattering wave and cannot be emitted before the arrival of the incident wave [10]. Great progress has been accomplished on analyze the dispersive in SOM for a wide range of nucleon scattering energy with different nuclei [11,12] and distinguish success in deriving SOM potentials on closed shell nuclei by [13-16] for which the experimental data for bound states are compared.

Optical model has been used to analyze the elastic scattering cross-section for p+ ^{40}Ca and predicted new optical parameters at proton energy range (9- 22 MeV) [17]. Also, the elastic scattering angular distribution of ^{58}Ni (^{4}He, ^{6}He) ^{56}Ni reaction have been studied by [18]. Different nuclear potentials are obtained with the phenomenological and the microscopic approach based on optical model.

The dispersion in potentials can be described by the nuclear mean field between the negative energy (bound state) and positive energy (scatter state). Then, it is able to fit the experimental nuclear probabilities more accurately than the simple optical model.

Theoretical background of SOM and DOM

The potential can be described by $v(r) + iw(r)$ where $v(r)$ is the real part of the potential and $w(r)$ is the imaginary part of the potential, where the elastic cross- section for potential scattering can be calculated by using SOM. The potentials are consisted of Saxon-Woods volume and surface derivation forms which can be described as [19]:

$$V_{op} = U_R(r) + iU_I(r) + U_{so}(r) \quad (1)$$

where $U_R(r)$, $U_I(r)$ and $U_{so}(r)$ are the real, imaginary and spin orbit potentials, respectively.

The real potential is assumed to have the Saxon-Woods form, and the imaginary potential is a surface Saxon-Woods derivation form. A spin orbit potential is in the Thomas form and the primary effect and it is the polarization of the scattered particle. The real potential is responsible for elastic scattering, while the imaginary potential is responsible for absorption. This potential can be written as follows [19]:

$$V_{op}(r) = -V_R f(x) - i[W_v f(x_{IV}) - 4W_D f'(X_{ID})] + \left(\frac{h}{m_0 c}\right)^2 V_{SO}(\bar{l}.\bar{\sigma})\frac{1}{r} f'(X_{SO}) \quad (2)$$

where V_R,W_v, W_D and V_{SO} are the real, imaginary volume, imaginary surface and spin-orbit potentials, respectively, $\left[\frac{h}{m_0 c}\right]^2$ is the square of pion-Compton wavelength, the quantity $(\bar{l}.\bar{\sigma})$ is the scalar product of the orbital and intrinsic angular momentum operators [20], f(x), f (X_{IV}), f (X_{ID}) and f (X_{SO}), are the radial dependent form factor for the real, volume, surface and spin-orbit terms respectively.

The form factors in Eq. (2) can be defined by Saxon-Woods form [19]:

$$f(r, R, a) = \left[1 + e^{\left(\frac{r-R}{a}\right)}\right]^{-1} \quad (3)$$

where R is the nuclear radius, $R = r_0 A^{1/3}$ and a is the surface diffuseness parameter.

It is expected that the low neutron energies attenuated near the surface of the target nucleus while the increasing in neutron energy caused more absorption for entire nucleus volume. For this the reason the SOM analysis deals with surface and volume absorption terms.

DOM can provided an analytic way of extrapolating the real part of the mean field from positive towards negative energies, by considering the prediction of single-particle bound-state and a self-consistent description of the energy dependence of the SOM, in particular near the Fermi energy. Furthermore, DOM imposes an additional constraint on the real and imaginary parts and thus reduces the obscurities in deriving the phenomenological optical parameters from experimental data [21, 22].

In the following dispersion relation treatment, the real central potential strength consists of a term $V_{HF}(r, E)$, Hartree-Fook potential and a correction depth potential term, $\Delta V(r, E)$:

$$V(r, E) = V_{HF}(r, E) + \Delta V(r, E) \quad (4)$$

where the depth of the dispersion term of potential $\Delta V(r, E)$ can be written as [22]:

$$\Delta V(r, E) = \frac{1}{\pi} P \int_{-\infty}^{\infty} \frac{W(r, E')\, dE'}{(E' - E)} \quad (5)$$

where $W(r, E')$ is the imaginary potential as a function of the scattering energy and can be expressed in terms of Saxon-Woods derivative form and P is the principle of the integral.

Since W(r, E') can be expressed in volume and surface terms, where the volume term represents the absorption potential while the other is the potential accompany around the Fermi energy of the target nuclei. Therefore, the volume dispersion term is given by:

$$V(r, E) = \frac{1}{\pi} \int_{-\infty}^{\infty} \frac{W(r, E')}{(E' - E)} dE' \quad (6)$$

And the surface dispersion term is given by:

$$W(r, E) = \frac{1}{\pi} \int_{-\infty}^{\infty} \frac{V(r, E')}{(E' - E)} dE' \quad (7)$$

One can noticed the integral in equation (6) should be analytical for a very restricted number of absorption potential energy dependence. Therefore, in order to consider the dispersive in potential it is assumed the $\Delta V(E)$ vanish at the Fermi energy E_f and can be written in the following form:

$$\Delta V(E) = \frac{p}{\pi} \int_{-\infty}^{\infty} W(E') \left(\frac{1}{(E' - E)} - \frac{1}{(E' - E_f)}\right) dE' \quad (8)$$

with the assumption that W (E) be symmetric with respect to the Fermi energy E_f, Eq. (8) can be expressed the form which is stable under numerical treatment namely [23]:

$$\Delta V(E) = \frac{2}{\pi} (E - E_f) \int_{-\infty}^{\infty} \left(\frac{W(E')}{(E' - E_f)^2} - \frac{W(E)}{(E' - E_f)^2}\right) dE' \quad (9)$$

where the dispersion term $\Delta V(E)$ is divided into two terms, $\Delta V_v(E)$ and $\Delta V_s(E)$, which arise through dispersion relation, Eq. (5) from the volume

$W_V(E)$ and surface $W_S(E)$ imaginary potentials, respectively.

To simplify present work the imaginary potential is energy independent using the definition of the SOM equation, where the real volume $V_v(E)$ and surface $V_s(E)$ central part of the DOM potentials are given by:

$$V_v(E) = V_{HF} + \Delta V_v(E), V_s(E) = \Delta V_s(E) \quad (10)$$

where V_{HF} (E) is a linear function of *E* for large negative E, and is an exponential for large positive E.

Following [24], the analyses of the optical potentials using the dispersion relations are not yet able to give any additional information, mainly because the phenomenological analyses in the high energy region are insufficiently accurate and extensive. They should considered the update improving data which is the only way for separating the real energy dependence of the observed optical potential and the spurious energy dependence introduced by the approximation of the non-local part by an equivalent local potential [19].

Results and discussion

Theoretical calculated of neutron elastic scattering cross section from ^{197}Au for energy range 1-20 MeV is achieved in the present work. The calculated differential scattering cross sections are compared with the experimental cross section data from EXFOR [23]. Various potential well depths of n-^{197}Au reaction have been investigated at different neutron energy, as shown in Fig.1. Where the imaginary part is described by Saxon-Wood form with energy-independent geometry parameters. In these analysis different types of absorption potentials have been considered, such volume plus surface, and volume plus surface absorptive potential. The diffuseness and radius of these potentials have been constant or to depend on the mass number. The energy dependence of the depth of the volume and surface terms of the imaginary potential is given by a Fermi-type function, and the parameters are adjusted to reproduce experimental data. In the case of the surface imaginary potential, the slow decrease of the volume integral at energies above the Fermi energy is assumed to reflect the gradual decrease of surface absorption with increasing energy, an observation confirmed in nucleon SOM analyses. The effect of the dispersive contributions of the imaginary volume and surface terms on the real potential both the depth and radial shape is affected. Where the real potential term full with increasing neutron energy while the imaginary potential term has a parabolic variation about the Fermi surface energy. For negative energies, the real potential deviates from regular behavior in the Fermis surface region due to DOM effect while the imaginary potential is attached to the fragmentation width of the target nucleus bound states. After optimize the OMP of the neutron induced elastic cross section of ^{197}Au has been calculated and evaluated at 1-20 MeV energy range, as shown in Table 1 and Fig. 2. The recommended cross section are in a good agreement with available experimental data. Now the neutron energy can be depended on integral (shape elastic, absorption and total cross section) for ^{197}Au heavy nuclei and calculated using the SOM optimization, which are reasonable and satisfactory for integral cross section prediction of ^{197}Au nuclei at energy below 20 MeV. The irregular behavior of this figure is the nucleus can be existed in a very large number of excited states, and if it is excited by the interaction the cross- section shows resonances whenever the incident energy is such that the energy of the compound system corresponds to that of one of the excited states of the

nucleus [25]. The SOM have been optimized through the minimization of chi- square per point, within the range (1.086×10^{-5}) for the range of target nuclei ($100 > A$ amu), and compared the calculated results with experimental data. The absorption cross section on imaginary part of the nuclear potential that takes into a count the absorption of the reaction flux from the elastic channel to the non-elastic is considered.

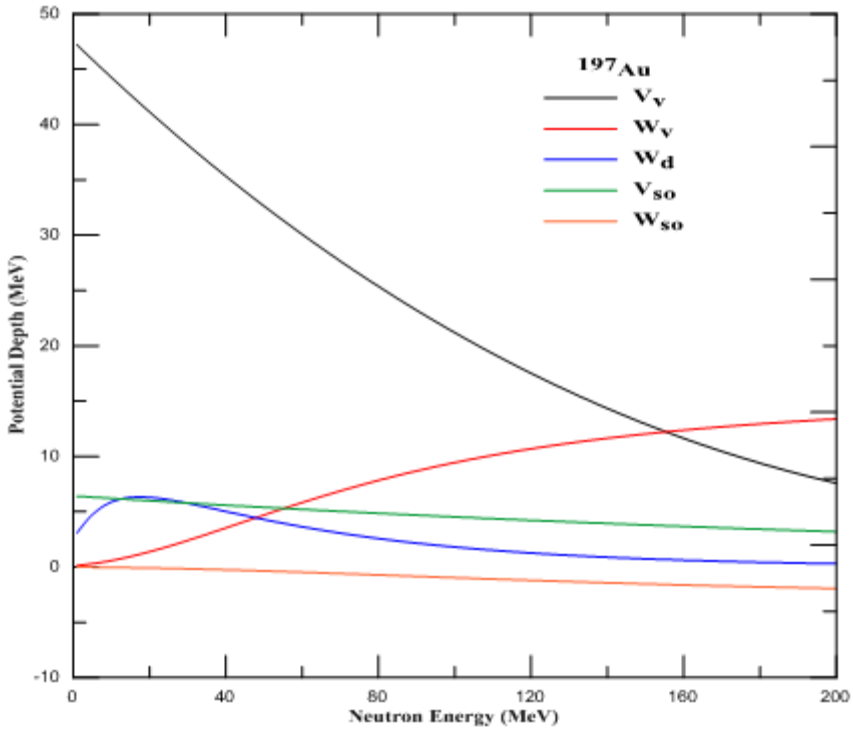

Fig. 1: The various potential well depths as a function of neutron energy incident for ^{197}Au nuclei.

Table 1: The present calculated total integral cross-section using SOM in ^{197}Au (n, n) ^{197}Au reaction at different energies compared with available experimental results.

E_N (MeV)	Total cross-section (b)	Experiential total cross-section(b) [26, 27]	Absorption (b)	Shape elastic (b)	Total compound (b)
5.293	6.94313	6.548	2.47238	4.4716	2.47153
6.027	6.40431	6.133	2.40284	4.00229	2.40201
7.003	5.76276	5.591	2.29823	3.40536	2.29741
8.055	5.24047	5.258	2.2824	2.95888	2.288159
9.082	5.0656	5.122	2.29781	2.70858	2.297
10.04	4.91195	5.076	2.2907	2.62202	2.28993
11.09	4.90877	5.106	2.25603	2.6535	2.25527
12.02	4.98448	5.169	2.23652	2.74872	2.23576
13.02	5.13617	5.247	2.23321	2.90372	2.23245
14.1	5.35171	5.37	2.24358	3.10889	2.24283
15.12	5.54819	5.461	2.24649	3.30245	2.24575
16.06	5.7137	5.557	2.22857	3.48587	2.22783
17.05	5.83127	5.629	2.20005	3.63195	2.19932
18.11	5.92371	5.68	2.16027	3.76416	2.15955
19.04	5.97998	5.704	2.13381	3.84689	2.13304

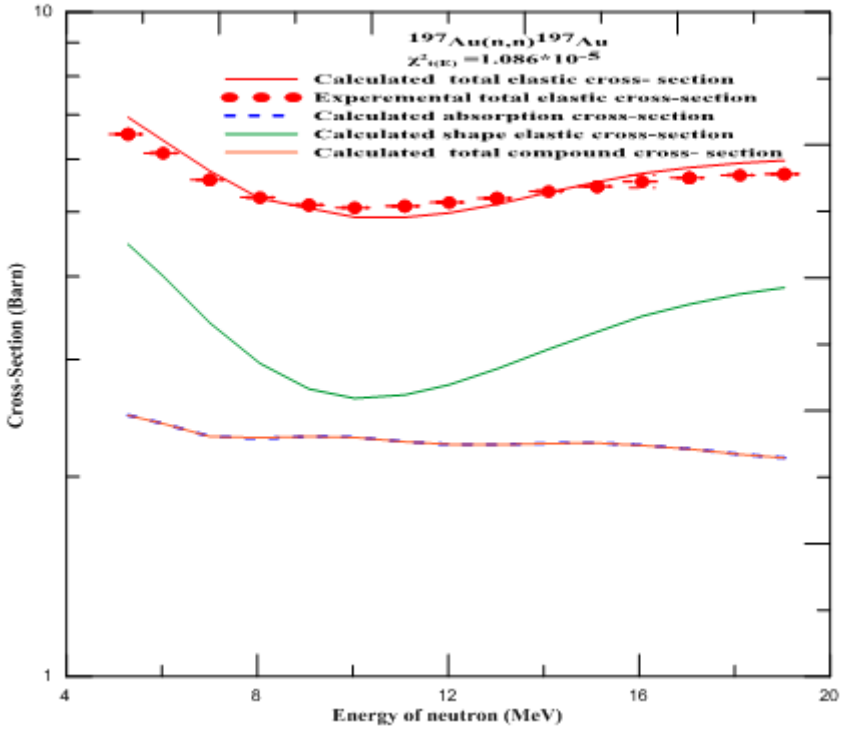

Fig. 2: The present calculated total Integral Cross-Section using SOM for neutron energy scattering on ^{197}Au nuclei at different energies compared with experimental data [26, 27].

Conclusions

1. The effect of the dispersive contributions of the real part decreases with increasing energy and the imaginary part has a parabolic variation around the Fermi surface energy.
2. It concludes that the surface imaginary strength fall linearly with energy concurrently where the volume imaginary strength increase linearly with energy.
3. Depending on Fig.2 the best fit of OMP is employed to calculate the integrated cross-section, absorption, shape elastic, total elastic and total compound cross-sections, of ^{197}Au(n, n) ^{197}Au reaction at different incident neutron energy (1-20 MeV). The comparison with experimental results show good agreement has been obtained for the total elastic cross-section with minimization of chi-square per point for reach within the range (1.086×10^{-5}).

References

[1] R. R. Roy and B. P. Nigam, "Nuclear physics theory and experiment", John Wiley and Sons, Inc. 1967.
[2] P. E. Hodgson, E. Gadioli and E. GadioliErba, "Introductory nuclear physics", Oxford University Press Inc., New York, second edition 1997.
[3] R. D. Serber, Phys. Rev., 72 (1974) 1008-1016.
[4] S. Fernbach, R. Serber, T. B. Taylor, Phys. Rev., 75 (1949) 1352-1355.
[5] P. G. Yong, "Optical Model Parameters", RIPL Handbook, 41 (1998).
[6] H. Feshbach, Ann. Phys., 5 (1958) 357-390.
[7] J. M. Cornwall and M. A. Ruderman, Phys. Rev. 128 (1962) 1474.
[8] C. Mahaux, H. Ngo, Nucl. Phys., A431 (1984) 486.
[9] J. W. Negele, E. Vogt (Eds), "Advances in nuclear physics",

Plenum, New York, 1991.
[10] C. Mahaux, H. Ngo, G. R. Satcher, Nucl. Phys. A449, 2 (1986) 354-394.
[11] G. Passatore, Nucl. Phys., A95 (1967) 694-704.
[12] R. Lipperheide and A. K. Schmidt, Nucl. Phys., A112 (1968) 65-75.
[13] C. Mahaux and R. Sartor, Nucl. Phys., A528 (1991) 253-297.
[14] C. Mahaux and R. Sartor, Nucl. Phys., A484 (1988) 205-263.
[15] W. Tornow, Z. P. Chen, and J. P. Delaroche, Phys. Rev. C 42 (1990) 693.
[16] C. Mahaux and R. Sartor, Nucl. Phys., A568 (1994) 1-51.
[17] M. M. Khalife, A. H. M. Solieman, M. N. H Comsan, Nucl. Phys., A 969 (2018) 83-93.
[18] M. Aygun, S. Cicek, Z. Aygun, I. Han, E. N. Han, Eastern Anatolian Journal of Science II, Issue II (2016) 49-52.
[19] P. E. Hodgson, "Nuclear reaction and nuclear structure" Book, Clarendon press, Oxford, 1971.
[20] A. J. Kang and J. P. Delarache, Nucl. Phys., A713 (2003) 231- 310.
[21] C. H. Johnson, D. J. Horen, C. Mahaux, Phys. Rev., C 36 (1987) 2252.
[22] C.H. Johnson, C. Mahaux, Phys. Rev., C 38 (1988) 2589- 2609.
[23] P. E. Hodgson, Contemporary Phys., 31, 5 (1990) 295-308.
[24] J. P. Delaroche and W. Toronw, Phys., Lett., B203 (1988) 4-8.
[25] R. D. Lawson and A. B. Smith, "A Neutron spherical optical statistical model Code-ABERAX", Argonne National Laboratory, ANL/NDM-145, 1999.
[26] R. Hannaske, Z. Elekes, R. Beyer, A. Junghans, D. Bemmerer, E. Birgersson, A. Ferrari, E. Grosse, M. Kempe, T. Koegler, M. Marta, R. Massarczyk, A. Matic, G. Schramm, R. Schwengner, A. Wagner, Jour: European Physical Journal A: Hadrons and Nuclei, 49 (2013) 137.
[27] W. P. Abfalterer, F. B. Bateman, F. S. Dietrich, R. W. Finlay, R. C. Haight, G. L. Morgan, Jour: Physical Review, Part C, Nuclear Physics, 63 (2001) 44608.